

INFLUENCE OF FAULTS ON ASCENT OF MAFIC MAGMA BY DIKE INTRUSION

Prepared for

**Nuclear Regulatory Commission
Contract NRC-02-93-005**

Prepared by

**Center for Nuclear Waste Regulatory Analyses
San Antonio, Texas**

October 1994



**INFLUENCE OF FAULTS ON ASCENT OF MAFIC
MAGMA BY DIKE INTRUSION**

Prepared for

**Nuclear Regulatory Commission
Contract NRC-02-93-005**

Prepared by

**Stephen R. Young
H. Lawrence McKague
Robert W. Terhune**

**Center for Nuclear Waste Regulatory Analyses
San Antonio, Texas**

October 1994

ABSTRACT

Faults and dikes are closely associated in the shallow crust. Physical or mechanical interaction between faults and dikes has been observed or postulated. Faults are commonly interpreted as having provided a conduit, or channel, for ascending magma. However, these interpretations have usually been based primarily on an observed close time and space association between fault traces and volcanic vents, or vent alignments, at the ground surface. Typically, the subsurface extent of the proposed fault/magma-conduit is not directly observable. For Quaternary volcanic systems especially, the key elements of the ascent process remain buried. Thus, key uncertainties persist concerning processes associated with occurrence of mafic volcanism and faulting in the central Basin and Range region. As reflected by the Key Technical Uncertainty topics included in the License Application Review Plan, these key uncertainties are particularly difficult to answer because doing requires information on subsurface conditions are not readily obtainable. Moreover, resolution of these uncertainties must encompass explanations for why, how, when, and where magmatism and faulting may occur together. Natural hazards that may be specifically related to interaction between faults and magmatic dikes are not directly included in the set of potentially adverse conditions in 10 CFR Part 60.122 but, will most likely be addressed during performance assessment. Quaternary basaltic volcanism is known to have occurred in the vicinity of Yucca Mountain and may have been as recent as Holocene in the case of Lathrop Wells Cone. Likewise, Quaternary movement has been documented on the Paintbrush Canyon, Bow Ridge, Solitario Canyon, Stagecoach Road, and Windy Wash Faults, as well as on numerous other northeast-trending faults in the vicinity of Yucca Mountain. The four Quaternary basalt centers, comprising the 1.2 Ma alignment of central Crater Flat Valley, form a northeast-trending, arcuate alignment that suggests control of surface location of vents in central Crater Flat by the northeast-trending fault system at Yucca Mountain. Lathrop Wells Cone may have formed along a splay of the northeast-trending Solitario Canyon Fault. Geological and geophysical mechanisms that controlled coupled or related mafic magmatism and faulting in the central Basin and Range region during the Quaternary are not well understood at time and space scales pertinent to performance assessment of a potential high-level waste repository. To help resolve key uncertainties, interaction of an upward propagating dike with an existing fault was simulated using the DYNA3D explicit finite element code. Three plane strain, relatively coarsely zoned models of fault-dike interaction have been completed. A 60° fault at a 1-km depth showed both the fault and the vertical dike opening around the intersection such that either path, or both paths, seemed likely to accommodate magma ascent. The calculation for an 80° fault at 1 km showed a slight opening of the dike a short distance past the intersection and a relatively large opening of the fault such that the fault seemed the more likely path for the magma. The calculation for the 80° fault at 300 m showed only the fault opening and, thus, the fault as the only possible path for the magma. Under environmental conditions specified for the dynamic models, faults that may be characterized as relatively simple contacts should be considered as potential conduits for magma ascent in the model depth range. Probability and consequence estimates for mafic magmatic processes should include models that accommodate magma transport along fault zones.

CONTENTS

Section	Page
FIGURES	iv
ACKNOWLEDGMENTS	v
1 INTRODUCTION	1-1
2 THEORETICAL MODELS OF FAULT CONTROL ON MAGMA ASCENT	2-1
2.1 60° FAULT AT 1 KM	2-2
2.2 80° FAULT AT 1 KM	2-6
2.3 80° FAULT AT 300 M M	2-9
3 FAULT CONTROL OF VOLCANISM AT YUCCA MOUNTAIN	3-1
3.1 FIELD OBSERVATIONS	3-1
3.2 IMPLICATIONS OF THE THEORETICAL MODELS	3-4
4 REFERENCES	4-1

FIGURES

Figure		Page
2-1	Vertical dike intersecting a fault dipping 60° (to the left) at a depth of 1 km (time step 11 sec)	2-3
2-2	Vertical dike intersecting a fault dipping 60° at a depth of 1 km (time step 15 sec)	2-5
2-3	Vertical dike intrsecting a fault dipping 80° at 1 km (time step 8)	2-7
2-4	Vertical dike intersecting a fault dipping 80° at a depth of 300 m (time step 12 sec)	2-8

ACKNOWLEDGMENTS

This report was prepared to document work performed by the Center for Nuclear Waste Regulatory Analyses (CNWRA) for the Nuclear Regulatory Commission (NRC) under Contract No. NRC-02-93-005. The activities reported here were performed on behalf of the NRC Office of Nuclear Material Safety and Safeguards (NMSS), Division of Waste Management (DWM). The report is an independent product of the CNWRA and does not necessarily reflect the views or regulatory position of the NRC.

QUALITY OF DATA, ANALYSES AND CODE DEVELOPMENT

DATA: There is no CNWRA-generated original data contained in this report. Sources for data should be consulted for determining the level of quality for those data.

COMPUTER CODE: The simulation documented in this report were performed using DYNA3D Computer Code by Integrated Parallel Technology Inc., a CNWRA subcontractor. The CNWRA does not have the DYNA3D code, and it's configuration is not controlled by CNWRA.

1 INTRODUCTION

The Nuclear Regulatory Commission (NRC) is required to review a license application from the U.S. Department of Energy (DOE) to construct and operate a proposed repository for high-level radioactive waste (HLW) at Yucca Mountain, Nevada. A key issue for compliance evaluation is whether a mined geologic repository at that location will provide effective post-closure isolation of the waste from the accessible environment in accordance with requirements set forth by the U.S. Environmental Protection Agency (EPA) in 40 CFR Part 191 and by the NRC in 10 CFR Part 60. Because of potential natural hazards related to volcanic processes and faulting in the vicinity of the proposed repository site, potentially adverse conditions that specifically relate to igneous activity, volcanism, and tectonic faulting have been included in 10 CFR Part 60: (i) evidence of igneous activity since the start of the Quaternary (i.e., within the last approximately 2 million yr) [60.122(c)(15) License Application Review Plan (LARP) 3.2.1.9]; (ii) structural deformation such as uplift, subsidence, folding, and faulting during the Quaternary Period, if characteristic of the controlled area or if it could affect isolation within the controlled area [60.122(c)(11) LARP 3.2.1.5]; (iii) structural deformation, such as uplift, subsidence, folding, or faulting that may adversely affect the regional groundwater flow system [60.122(c)(4) LARP 3.2.2.8]; and (iv) potential for changes in the regional ground water flow system and resultant adverse effects on repository performance induced by large scale surface water impoundments due to volcanic activity [60.122(c)(3) LARP 3.2.2.7].

Furthermore, EPA standards for release of radioactivity require assessment of waste isolation performance of the proposed HLW repository for a period of 10,000 yr. Based on the EPA standards, the overall system performance objective for a geologic repository (10 CFR 60.112 LARP 6.0) imposes limits on post-closure cumulative releases of radionuclides. Tectonic and magmatic processes, such as faulting, and magmatic dike intrusion and vent eruption has the potential of substantially influencing long-term (postclosure) performance. Thus, detailed information on the Quaternary geological features of the site, such as type, distribution, and age of faults, dikes and vents, that may affect repository design or performance, is required to be included in the Safety Analyses Report (SAR) of the license application [10 CFR 60.21(c)(1)]. The SAR [10 CFR 60.21(a)] generally will include a description and assessment of the proposed repository site. Where subsurface conditions outside the controlled area may affect isolation within the controlled area, the site description must also include that information, [60.21(c)(1)(i)]. Detailed information required in the SAR includes data on the distribution and characteristics of other potential pathways such as solution features, breccia pipes, or other potentially permeable features; and the geomechanical properties and conditions, including pore pressure and ambient stress conditions [60.21(c)(1)(i)(A)(B) and (C)]. Required assessments, as described in 60.21(c)(1)(ii)(A)-(F), should include analyses of the geology, geophysics and hydrogeology, and analyses and evaluations of favorable and potentially adverse conditions, post-closure performance, and the effectiveness of natural barriers.

Natural hazards that may be specifically related to interaction between faults and magmatic dikes are not directly included in the set of potentially adverse conditions (PACs) in Section 60.122 but, rather, will most likely be addressed during performance assessment (PA). However, given the characteristics of the geologic setting, certain potentially adverse conditions, as described in 10 CFR Part 60, anticipate the potential effects of combined faulting and dike intrusion. Yucca Mountain lies within a region in which both faulting and mafic volcanism have occurred widely throughout the late Neogene and more locally during the Quaternary. Moreover, the primary mechanism for ascent of mafic magma in this region is generally interpreted to be predominately upward (with some lateral) propagation of dikes. Section 60.122(c)(4), for example, addresses the potential for changes in ground water flow due to the presence, or development, of faults. The hydrogeologic properties of existing faults and fracture systems could be

altered substantially, by intrusion of magma along the fault surface. The hydrogeology of a fault, or fracture system, may also be altered significantly, but more locally, where a magmatic dike cross-cuts the fault zone. Key technical uncertainties (KTUs) that are common to tectonic and magmatic processes at Yucca Mountain, and important to PA, include: (i) an inherent inability to clearly resolve or detect faults, magmatic dikes, and buried volcanic vents [LARP 3.2.1.9 (Type 4)]; (ii) an inability to sample igneous features [LARP 3.2.1.9 (Type 5)]; and (iii) development and use of conceptual tectonic models as related to igneous activity and tectonic deformation [LARP 3.2.1.9 and 3.2.1.5 (Type 5)]. Thus, discerning the role of faults as conduits or guides for magma ascent in the Yucca Mountain area is left almost completely to modeling and indirect inference based on surface geologic and geophysical investigations.

Connor et al. (1993) have discussed the implications of lateral transport of magma by faults for eruption probability and consequence calculations. Ho (1992) and Connor and Hill (1993) illustrate the reliance of eruption probability models on estimates of distribution and timing of dike intrusion and vent eruptions in the Yucca Mountain region. Because the *in situ* stress state strongly influences the distribution and geometry of dikes, associated vent eruptions are nonrandom. Fault control of lateral subsurface magma transport and focusing of vent eruptions along, or adjacent to, the ground-surface trace also results in nonrandom intrusion and eruption patterns. Eruption probability estimates should, therefore, specifically include models in which faults serve as transport conduits and in which eruptions are localized along fault traces. Such models require estimates of the range of intrusion depth and fault dip over which the fault surface may serve as a conduit, or guide for ascending magma. Intrusion depth, fault dip, and dip direction (azimuth) largely determine the capture area, that is, the area over which faults may serve as effective conduits. Analyses presented in Section 2 assume faults dipping in the direction of minimum horizontal stress.

Key uncertainties persist concerning processes associated with occurrence of mafic volcanism and faulting in the central Basin and Range region. As reflected by the KTU topics listed previously, these key uncertainties are particularly difficult to answer because to do so requires information on subsurface conditions that is not readily obtainable. Moreover, resolution of these uncertainties must encompass explanations for why, how, when, and where magmatism and faulting may occur together. The requisite phenomenological explanations and supporting subsurface data bear directly on the ability to assess time and space patterns of volcanism, and consequent likelihood of volcanic or magmatic activity at a given location. Important geological issues (and associated key uncertainties) that should be addressed to properly assess timing and distribution of magmatic and volcanic activity in the Yucca Mountain area include: (i) relationships between subsurface magmatic processes, surface eruptive processes, and structural position within the extant fault systems; (ii) influence of the contemporary stress and strain field; and (iii) the interplay between magma supply characteristics (depth, volume, and rate) with contemporaneous faulting.

2 THEORETICAL MODELS OF FAULT CONTROL ON MAGMA ASCENT

Geological faults and magmatic dikes exist together in the shallow crust of the earth. A variety of styles of interaction between faults and dikes has been observed or postulated. In particular, faults are commonly interpreted as having provided a conduit, or channel, for ascending magma. However, these interpretations have usually been based primarily on an observed time and space association between fault traces and volcanic vents, or vent alignments, at the ground surface. Most often, the subsurface extent of the proposed fault/magma-conduit is not directly observable. For Quaternary volcanic systems especially, the key elements of the ascent process remain relatively deeply buried.

With respect to Yucca Mountain, the geological features of interest in this analysis are mafic dikes and the set of extant normal, normal-oblique to strike slip faults. This analysis is primarily concerned with the interaction of ascending mafic magma with pre-existing faults. The interaction was initially envisioned to occur essentially as one of three relatively discrete end member styles: (i) no effects — propagation of the dike through the fault with no diversion of magma; (ii) the fault acts as a magma conduit — at least some of the magma flows into the fault zone and travels for some distance laterally as a result; and (iii) a strong impermeable fault zone acts as a magma guide — magma does not enter the fault zone, but rather is blocked against the underside of the fault zone and ascends through the crust adjacent to the fault zone. The important question is, under what conditions can each of these styles be expected to dominate the dike-intrusion process? The models developed during this study are preliminary in that a more comprehensive range of parametric studies could be conducted. However, considerable insight has been gained with respect to parameters that influence propagation of vertical dike fractures versus flow of ascending magma into extant fault zones. Indeed, an alternative composite style was identified that had not been initially considered. The composite style (iv) is a simple mix of (i) and (ii) — magma flows into and along the fault interface and at the same time continues to propagate upward along a vertical dike fracture, that propagates in advance of the intruding magma.

The interaction of an upward propagating dike with an existing fault was simulated using the DYNA3D explicit finite element code (Whirley and Hallquist, 1991). Three plane strain models have been developed of an upward-propagating vertical dike intersecting: (i) a fault dipping 60° at a 1-km depth; (ii) a fault dipping 80° at a 1-km depth; and (iii) a fault dipping 80° at a 300-m depth. The dike was modeled as a magma-driven extension fracture composed of adjacent surfaces (contact elements) that required development of a threshold tensile stress to separate. Magma moving upward along the opening extension fracture was modeled by a propagating time-dependent pressure profile. For these models, the rise time of the pressure is independent of depth. The upward-traveling pressure pulse, applied to the fracture interface, causes the fracture to propagate as the pressure exceeds the strength of the media. The fault was modeled as a simple interface. Cohesion and friction on the fault are minimum values used only to prevent slip under the simulated gravitational load.

A number of methods were tested for computing the initial overburden stress state (confining pressure). The method chosen for the initial series of simulations is a boundary pressure method. With application of the boundary loads, the entire grid is allowed to undergo dynamic relaxation to ensure all zones are in stable equilibrium. Horizontal boundary loads are balanced to prevent the grid from deforming under the burial stress. For simplicity, the models thus far have assumed an elastic media with a density of 2.7 to 2.4 gm/cm^3 , a Poisson's ratio of 0.2 , and compressional velocities of 6.1 to 3.4 km/sec . At a depth of 1 km , the overburden pressure is about 0.025 GPa . Under these conditions, a simulated magma pressure of

approximately 0.37 GPa is required to open an extensional dike fracture about 0.75 m. Connor et al., (1994) conducted an analytical parametric study that indicated magma pressure values between approximately 9 and 23 MPa are required to open a dike fracture to a width of about 1 m. Dike width estimates are based on field observations (Connor et al., 1994). They determined that a pressure of approximately 16 MPa would be reasonable under realistic conditions at confining pressure=25 MPa (depths between about 1 and 2 km). These magma pressure estimates are consistent with pressure versus depth curves calculated by Parsons and Thompson (1991; 1993). Pollard (1987) determined that magma-driving pressure, the difference between magma pressure and the minimum horizontal stress, needed to be at least 1 to 4 MPa, but could be as high as several tens of MPa, depending on host rock strength. Pollard and Segall (1987) concluded that a driving pressure in excess of 5 MPa was required for the dike fracture to propagate to the ground surface. For mafic magmatism throughout the Eastern Snake River Plain, Kuntz (1992) determined that magma pressures in the range of 10 to 20 MPa are realistic. Kuntz estimates are based on magma chamber depth and buoyancy.

2.1 60° FAULT AT 1 KM

The simulation grid is divided into distinct material blocks that are individually zoned, with each block having its own individual boundary condition and initial condition. The dike and fault intersection was modeled with four blocks joined together by slip lines (Figure 2-1). The block to the left of the dike and in the footwall (below) of the fault, and the block to the right of the dike and in the hanging wall (above) of the fault were both divided again into two separate vertical sections. This procedure was done to maintain a relatively close grid node spacing along the entire length of the dike. These six blocks define the model grid in the area 27 m on either side of the dike. Two larger blocks define the model grid in the area from 27 to 140 m on either side of the dike. The depth at the top of the grid is 1,019.4 m, the depth at the dike-fault intersection is 1,080 m, and the bottom of the grid is at a depth of 1,140.6 m.

The dike fracture interface was bonded together with a tensile strength of 0.02 Gpa (200 bars). The tensile strength of the dike (200 bars) is approximately 0.16 to 0.20 of the dike pressure required to open the dike fracture against the normal stress and the stiffness of the confining media. A pressure pulse with a rise time of 500 msec and a peak pressure of 0.1 GPa was run up the dike surface from the bottom of the grid to the intersection of the dike with the fault at a velocity of 5 m/sec. The fault has a coefficient of friction of 2.0 to prevent the 60° fault from slipping under the gravity load. The overburden was modeled as a simple lithostatic pressure with an average overburden density of 2.6 gm/cm³. The calculations are two dimensional, in plane strain configuration, where no displacement or strain normal to the grid was allowed. In all the figures, the y-axis is vertical, the x-axis is horizontal, and the z-axis is normal to the view-plane.

The material properties for the calculations were based on laboratory measurements of a sample of dolomitic limestone from borehole U7ae, located near Yucca Mountain in the Yucca Flats area of the Nevada Test Site (Van Burkirk et al., 1978). The sample was taken from a depth of 2,850 ft (867 m). The sample bulk density as received was 2.69 gm/cm³; the dry sample density was 2.64 gm/cm³. Poisson's ratio determined from measured sonic velocities (V_p - longitudinal=6.13 km/sec; V_s =3.19 km/sec) is 0.314. Data from uniaxial strain tests on these samples were used to constrain pore compaction along the dike to approximately 1 percent. Rock strength estimates were made from triaxial tests at confining pressures of 0.0 (unconfined), 0.05 and 0.4 GPa (Van Burkirk et al., 1978). Based on the triaxial test data two shear stresses (rock strengths) are possible, a higher shear stress of 0.7 GPa and a lower shear stress of 0.35 GPa. The lower value was used for this calculation, initially to account for a reduction in the

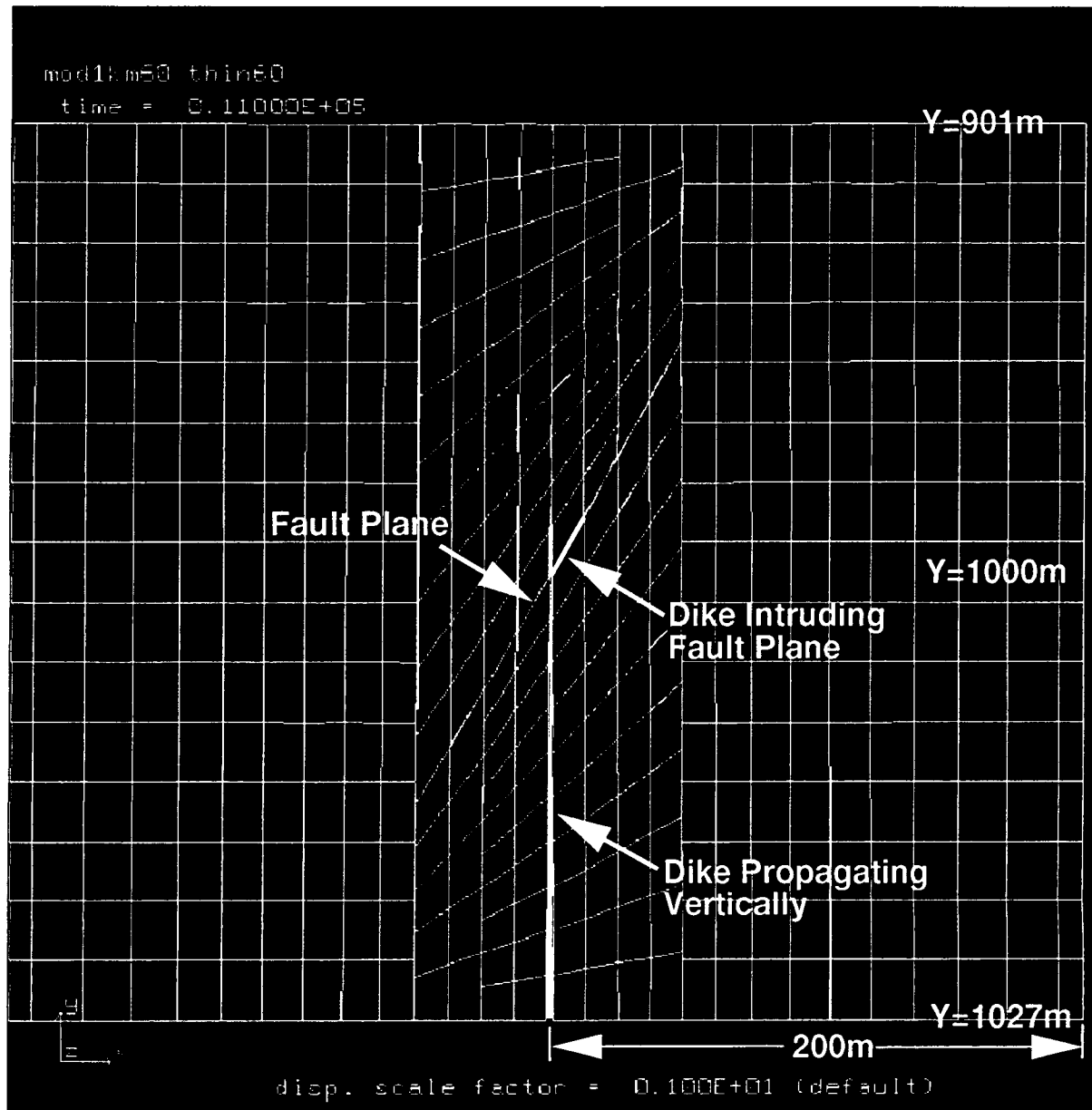


Figure 2-1. Vertical dike intersecting a fault dipping 60° (to the left) at a depth of 1 km (time step 11 sec). At the intersection, both the dike and the fault are open. For clarity open dike and fault have been enhanced.

strength of the rock along the dike due to the high temperature of the magma. However, some additional background work needs to be done to document the temperature dependence of strength in this temperature range. The higher strength estimate may be more appropriate if thermal weakening is restricted to a narrow zone immediately adjacent to the dike, or if temperature dependent ductility results in strengthening.

The key criterion for setting the dike pressure was that the dike fracture should be forced open about 1 m horizontally, and 0.5 m in both the positive and negative x-directions. In order for the calculations to show the dike opening and remaining open with minimum grid distortion an initial parameter study was required in which only the dike was modeled. The velocity of the pressure was set at 100 m/sec to speed up the calculations. Actual ascent velocities are expected to be as high as approximately 1 cm/sec (Petford et al., 1993); however, Emerman and Marrett (1990) suggest that at least 1 m/s is required for entrainment of xenoliths.

The simulation showed that within the blocks directly adjacent to the dike, distinct regions of compression are quickly developed. A region of tension is well developed ahead of the pressure pulse. The pressure pulse was confined to approximately the lower two thirds of the grid, but the dike propagated vertically through the entire block. The peak pressure occurred at the bottom of the grid at 0.5 sec and reached the end of its travel at 1.5 sec. The top third of the dike remains in tension for several seconds and eventually breaks apart to allow the dike fracture to open throughout the entire block. In the faulted-model cases, the calculation was terminated before the break occurred. Repeated calculations for the 1 km depth case indicated that a magma pressure of approximately 0.1 GPa was required to open the dike fracture to a width of 1 m.

Stress and displacement were calculated in the x (horizontal) and y (vertical) directions at each time step. Calculations of horizontal displacements show that the dike had a maximum growth of about 1 m. This dike growth is a key parameter that could play an important role in determining if an intersected fault will open before the dike crosses the fault and propagates into the material above the fault. Application of overburden stress, acting in the y-direction, resulted in a small settling at the top of the grid of approximately 5 cm. The pressure at the bottom of the dike initially caused a small upward displacement of about 1 cm at the bottom of the grid. However, the lower surface of the grid is held as a fixed boundary, which allows no displacement in the vertical direction. The pressure pulse, as it moves up the dike fracture with time, is best expressed in the horizontal stress gradient. At full dike width (approximately 1 m), the horizontal stress is predominately just under the overburden load. The vertical stress calculations also show the compressive pulse as it moved upward along the dike fracture. The vertical stress became slightly tensile ahead of the pressure pulse. At 5 sec, the vertical stress around the leading tip of the dike fracture was tensile. At the same time, the vertical stresses along the upper part of the dike, but behind (below) the tip, are slightly less than overburden. From 7 to 9 sec, the tensile stresses seem to intensify both along the dike and within the region of dike-fault intersection. At 11 sec, the tensile stresses are well developed along both sides of the dipping fault, while vertical stresses along the dike are still slightly compressive. At 12 to 14 sec, vertical tensile stresses are decreasing around the fault but intensifying on the dike fracture above the fault. Vertical stress levels outside of the blocks directly adjacent to the dike are approximately at overburden.

At 9 sec, the fault is just beginning to open slightly while the dike above the fault remains closed. At 11 sec, (Figure 2-1) the up-dip side of the fault is clearly open, and the dike above the fault is beginning to break open. At 13 sec, the fault is beginning to close slightly, while the dike fracture seems to be opening in four places (discontinuously) above the fault. By 15 sec (Figure 2-2), the dike

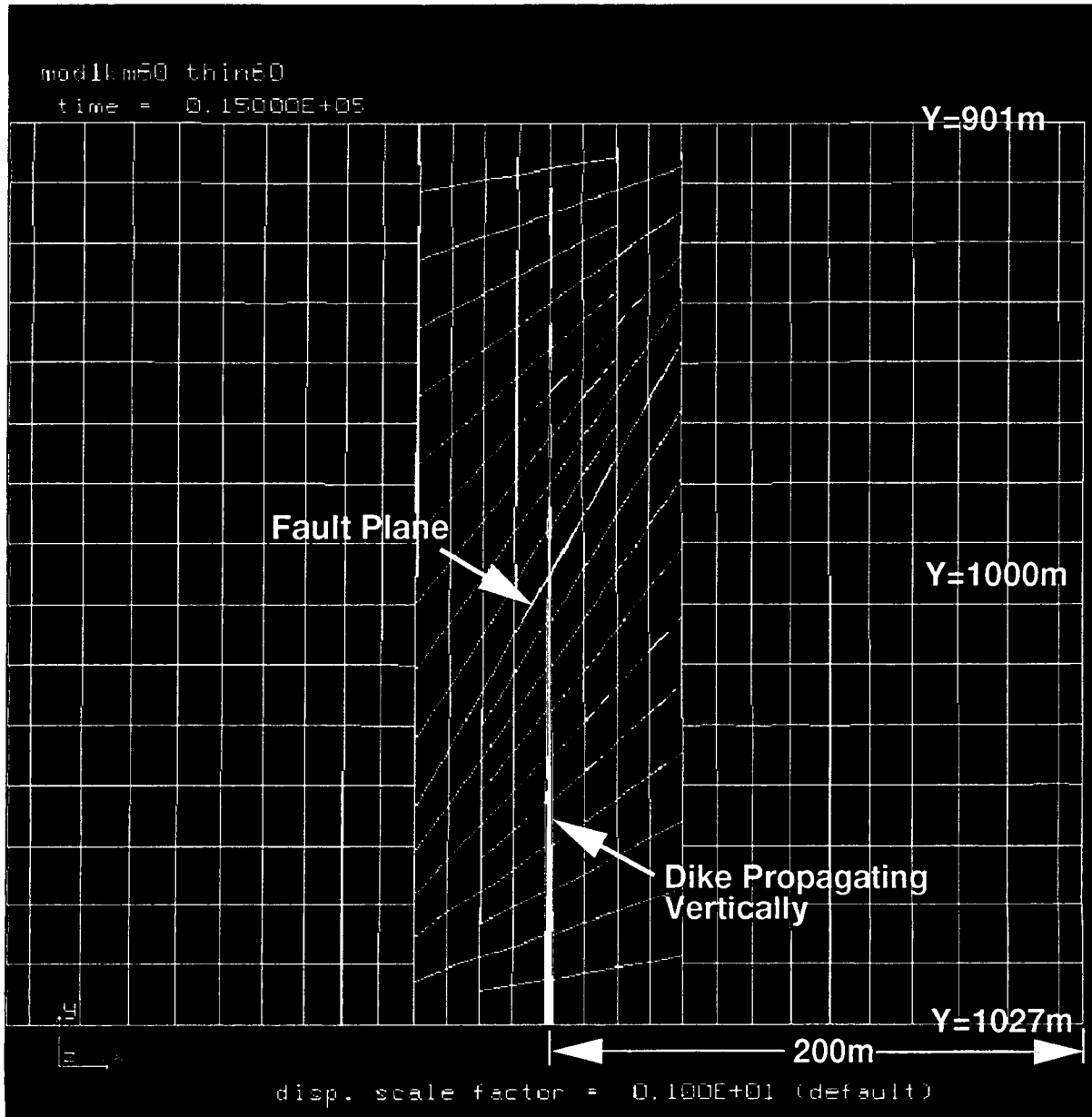


Figure 2-2. Vertical dike intersecting a fault dipping 60° at a depth of 1 km (time step 15 sec). Dike is well advanced past the intersection point. For clarity open dike and fault have been enhanced.

above the fault is open in isolated spots. Whether the magma would travel exclusively up the fault, or continue on past the fault and up the dike fracture can not be determined from this one calculation. Variable parameters that have an important influence on the combined behavior of this type of system include compressive and tensile strength of the host rock, compressibility of the host rock, and the width of the dike opening. This calculation shows that under realistic environmental conditions, meaningful results are obtained that indicate both the fault and the dike fracture above the fault can open and provide a magma conduit. The down-dip side of the fault (to the left of the dike) apparently played no role in either the development of the fracture above the fault nor the opening of the fault on the up-dip side.

2.2 80° FAULT AT 1 KM

In these simulations, only the up-dip side of the fault was modeled to simplify the zoning (Figure 2-3). The grid spans the depths of 901 to 1027 m and is 400 m wide. Figures 2-3 and 2-4 show the more finely zoned region 54 m on either side of the dike. The more coarsely zoned bounding blocks that extend to the model edges are not shown. As before, the dike fracture interface was bonded together with a tensile strength of 0.02 GPa. The static and kinetic coefficient of friction of the fault is 2.0. The magma was modeled with a pressure pulse that traveled upward along the dike fracture interface from the bottom of the grid to the intersection with the fault at a velocity of 5 m/sec. The pressure of the pulse was 0.13 GPa. The overburden was modeled as a lithostatic (hydrostatic) pressure with an overburden density of 2.6 gm/cm³, which gives a confining pressure of approximately 0.025 GPa. The material properties for this calculation are the same as for the 60° at 1-km simulation in Section 2.1. This calculation was run to 9 sec.

At 3 sec, an abrupt horizontal stress gradient has developed near the bottom of the grid as the tip of the dike fracture begins to propagate into the grid. Horizontal stress is approximately equal to overburden throughout the top half of the grid. The dike fracture intersects the fault at 5 sec. At 6 sec the strong horizontal compression pulse has just reached the dike-fault intersection and the dike fracture continues to widen below the fault. The horizontal stress field stabilizes at 8 sec. The dike width grows from approximately 0.3 m at 3 sec, to a maximum total width of 0.9 m at 8 sec. The relatively low-tensile strength of the dike fracture allows the fracture to open several zones ahead of the pressure pulse. As in the previous calculation, the vertical stress distribution shows both the compressive stresses around the dike pressure pulse and the tensile stresses ahead of the pressure pulse. At 3 sec the vertical stress in the region above the intersection of the fault and the dike is approximately equal to overburden, but with time becomes more tensile. By 5 sec both the fault and the dike have opened slightly, while the dike pressure pulse is still approximately 8 m from the intersection. At 6 sec the dike fracture above the fault begins to break open. At 8 sec vertical stress is tensional around both the fault and the dike fracture above the fault, and both the fault and the higher level dike are open. Vertical tensile stresses built from 12.5 bars to an approximate peak of 100 bars during the period from 5 to 7 sec. At 7 sec the dike has opened along a distance about 8 m above the intersection. The fault, however, is open to about 35 m above the intersection (Figure 2-3).

The 80° fault opened up considerably more than the 60° fault and the dike opened much less. This difference in opening suggests that the 80° fault would provide a more accessible path for magma ascent than the 60° fault at the same depth. The distance ahead of the pressure pulse that the dike fracture propagates is dependent on the tensile strength across the dike and the leverage effect acting across the pressurized dike fracture interface. Thus, the tensile strength across the dike is an important parameter in determining if the magma would continue vertically upward or be diverted by the fault. The 200 bar

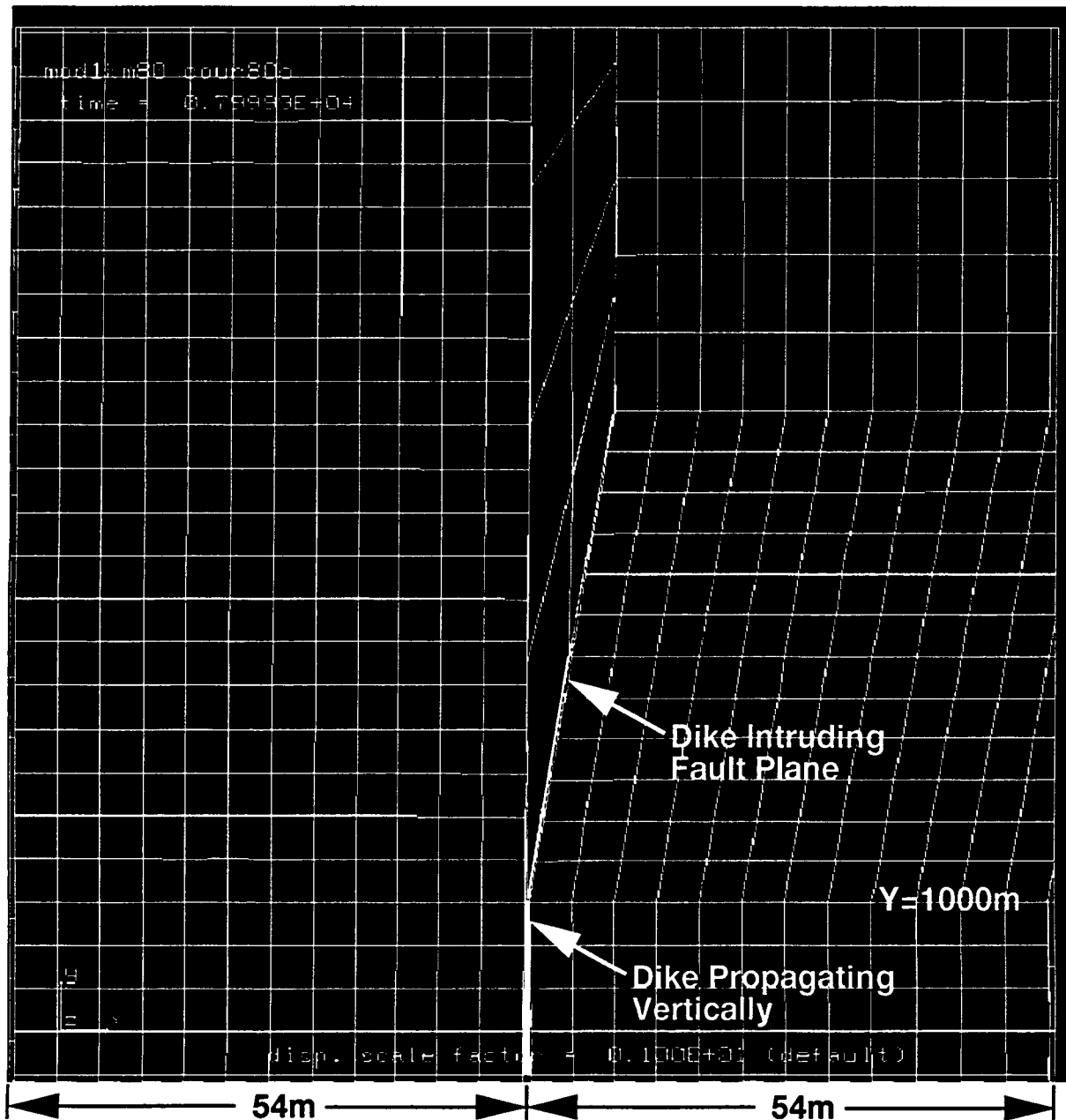


Figure 2-3. Vertical dike intersecting a fault dipping 80° at 1 km (time step 8 sec). At the intersection, both the dike and the fault are opened by the magma pressure. For clarity open dike and fault have been enhanced.

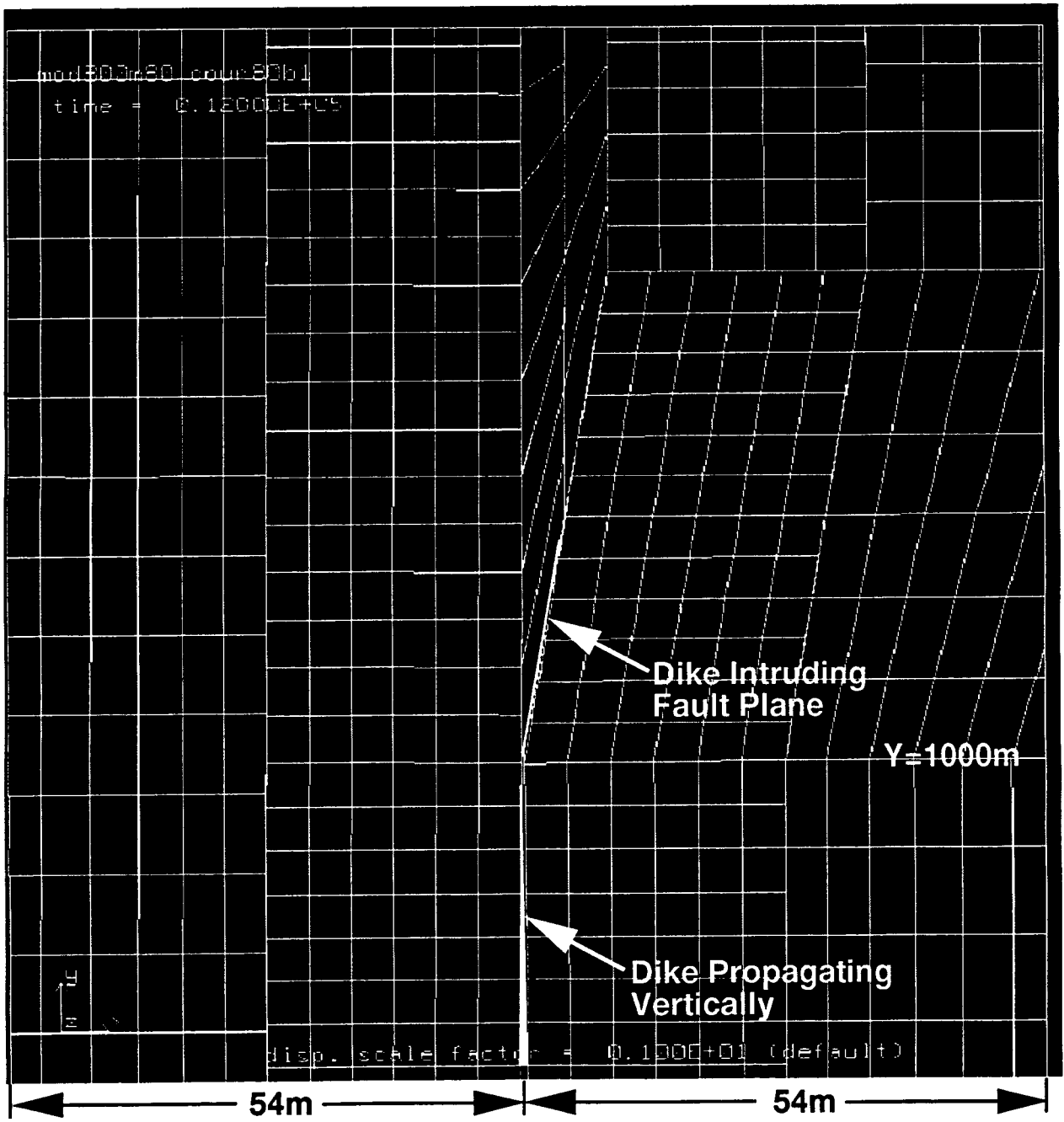


Figure 2-4. Vertical dike intersecting a fault dipping 80° at a depth of 300 m (time step 12 sec). The fault is opened by the magma pressure, and the dike stops at the fault. For clarity open dike and fault have been enhanced. For clarity open dike and fault have been enhanced.

tensile strength used in these calculations seems to be near the threshold that would separate one path preference from the other at this depth.

2.3 80° FAULT AT 300 M

The grid for the 80° fault model at a depth of 300 m is essentially the same as the one described above at 1 km (Figure 2-4). The fault dike intersection is at 300 m (Figure 2-4), with the top and bottom of the grid at depths of 220 m and 336 m, respectively. The total width of the grid is 280 m. The fine zoning is 27 m on each side of the dike. The pressure of the magma was 0.026 GPa. The overburden density was 2.4 gm/cm³ which gives a confining pressure of approximately 0.006 GPa. The material properties for the 300 m calculation are based on measurements of volcanic tuff from borehole Ue4b at the Nevada Test Site. The sample bulk density was 2.12 gm/cm³ with 11.4 wt% water. Poisson's ratio based on sonic velocities was calculated at 0.337 ($V_p=3.37$ km/sec; $V_s=1.67$ km/sec).

Throughout the time series of this set, the upper half of the grid remained at the overburden stress. The pressure pulse (at 5 m/sec) takes approximately 8 sec to reach the intersection of the dike and the fault. The peak dike pressure pulse (magma pressure) was 0.026 GPa, which added to the confining pressure due to overburden, and gives the peak horizontal stress adjacent to the dike. The dike width grows slowly to a maximum of 0.73 m at 12 sec (Figure 2-4). This width is slightly less than the calibration calculations give. The calibration calculations end with the dike pressure acting over 100 m of dike surface versus the 36 m of dike surface area in this calculation. There seems to be a significant leverage effect on the extent of the dike which most likely accounts for the dike fracture tip running several zones ahead of the pressure pulse. The dike pressure is only slightly greater than the 0.02-GPa tensile strength assigned to the dike fracture. At 5 sec the fault has opened and vertical tensile stresses are beginning to develop across the dike above the intersection. The peak pressure was still several zones (grid cells) below the intersection. At 7 sec the fault continued to open, and peak vertical tensile stress is developed across the dike fracture. This condition holds steady to 12 sec (Figure 2-4) as both the fault and the dike fracture below the fault continue to widen.

The tensile strength of 200 bars across the dike above the intersection was not exceeded and the dike remained tightly closed (Figure 2-4). The fault opened approximately 0.3 m at the intersection, remaining closed beyond the point at 20 m past the intersection. For this calculation, the fault seems clearly to be the preferred path for magma ascent.

3 FAULT CONTROL OF VOLCANISM AT YUCCA MOUNTAIN

The processes that controlled mafic magmatism and volcanism in the central Basin and Range region during the Quaternary are not well understood at time and space scales pertinent to PA of a potential HLW repository. Quaternary basaltic volcanism is known to have occurred in the vicinity of Yucca Mountain (Crowe, 1990; Smith et al., 1990; Champion, 1991; Turrin and Champion, 1990) and may have been as recent as Holocene in the case of Lathrop Wells Cone (Crowe, 1990). Consequently, uncertainties persist about the potential for renewed subsurface magmatic or volcanic activity in the Yucca Mountain area, and the potential for disruption of a repository at Yucca Mountain.

3.1 FIELD OBSERVATIONS

The central Basin and Range region evolved during a period of strong crustal extension which occurred principally during the last 15 million yr (Kruse et al., 1991; Wernicke et al., 1988). Spatial and temporal patterns of Cenozoic extensional deformation of the central Basin and Range region are not well known, and considerable uncertainty exists as to how accumulated deformation, resultant faulting, and associated magmatism are related. Wernicke et al. (1988) determined that 247 km (± 56 km) of extensional displacement has been accommodated between the Colorado Plateau and the Sierra Nevada Range during the last 15 million yr. The total relative separation is distributed along a net vector of about N73W ($\pm 12^\circ$) between two distinct highly extended terrains separated by a relatively unextended domain. The Yucca Mountain area is within the western-most of the highly extended regions, referred to as the Death Valley normal fault system by Wernicke et al. (1988). Average extension rates in the Death Valley normal fault system varied from an estimated maximum of 20 to 30 mm/yr between 15 and 10 million yr ago to a diminished rate of less than 10 mm/yr over the last 5 million yr (Wernicke et al., 1988). Magmatism is commonly associated with extension and normal faulting throughout the central Basin and Range region and is most often directly associated with strongly extended terranes.

Two general styles of extensional faults are developed in the central Basin and Range region: (i) low-angle detachment fault systems, described by Coney (1973) in connection with development of extensional metamorphic core complex terranes of the North American Cordillera, accommodate large-magnitude extensional strain, and (ii) deeply penetrating, high-angle fault systems, often referred to as domino-style faults, are widely interpreted to be the mechanism of classical Basin and Range physiography (e.g., Stewart, 1984; Okaya and Thompson, 1986; Allmendinger et al., 1987), but do not accommodate large extensional displacements.

Scott and Bonk (1984) mapped a series of northeast trending, west-dipping normal faults that both bound and occur within the potential repository block. Scott and Bonk (1984) also mapped a series of northwest-trending strike-slip faults that occur in the northeastern part of Yucca Mountain. Scott (1990) interprets the northeast-trending, west-dipping faults as normal faults having a listric geometry at depth based on the geometry of related deformation observed in the hanging wall blocks. Two-dimensional modeling of the structures at Yucca Mountain using the data of Scott and Bonk (1984) and computer-assisted cross-section balancing methods (Young et al., 1993) indicates that the interpretation of the faults as listric normal faults, which flatten and merge into a detachment surface at depth, is geometrically reasonable. Scott (1990) reports that offset on the northeast-trending normal faults generally increases southward along strike of the fault system. For example, the Solitario Canyon fault branches into four major splays over a distance of approximately 10 km and cumulative offset increases from zero in the north to approximately 1 km at its southern end.

Quaternary movement has been documented on the northeast-trending Paintbrush Canyon, Bow Ridge, Solitario Canyon, Stagecoach Road, and Windy Wash faults, as well as on numerous other northeast-trending faults in the vicinity of Yucca Mountain (Swadley et al., 1984). Northeast-trending faults in the central and southern parts of Yucca Mountain display only minor oblique to horizontal slip. The greatest lateral displacement occurs along the Stagecoach Road Fault, with 5 to 7 m of left lateral offset of washes in Quaternary fan deposits (Scott and Whitney, 1987). The Stagecoach Road Fault is interpreted by Scott (1990) to project into the Paintbrush Canyon Fault to the northeast. However, Scott (1990) reports that no Quaternary movement has been identified on any of the northwest-trending faults, including those in the northeast part of Yucca Mountain in the vicinity of Yucca Wash. One of the faults exhibiting Quaternary displacement is the east-dipping Bare Mountain Fault, which bounds Bare Mountain on the east flank (Reheis, 1986). This structure is located west of Yucca Mountain and is interpreted by Scott (1990) as a deep-seated normal fault that cross-cuts a low-angle detachment surface that dips westward beneath Yucca Mountain. Hamilton (1988) has interpreted the Bare Mountain Fault as an eastward dipping detachment.

Scott (1990) indicates that fault movement can be placed within the following five general time brackets: 14–13.5 Ma, 13.5–13 Ma, 13–11.5 Ma, 11.5–1.7 Ma, and 1.7 Ma to present. These periods also bracket the times suggested by Carr (1984) for fault slip. Scott (1990) indicates that bracketing fault slip in this way provides little support for models of episodic faulting which attempt to temporally relate extension, faulting, and volcanism in a general way. Estimated age brackets for faulting are not narrow enough, or precisely enough defined to correlate with distinct episodes of mafic volcanism. The episodic model of Cenozoic extensional deformation described by Scott (1990) is based on the assumption that some type of genetic link exists between crustal extension, fault movement, and volcanism in the Yucca Mountain area. In the episodic model, a hiatus in fault movement is assumed to causally coincide with a hiatus in volcanism in the Yucca Mountain area between about 10 and 4 Ma. In contrast, Parsons and Thompson (1993) propose that dike injection should suppress normal faulting. Thus, increasing volcanism would coincide with a hiatus in faulting. With renewed volcanism around 3.7 Ma faulting may have decreased. Scott (1990) indicates that fault slip at Yucca Mountain is consistent with a stepwise decreasing rate model of extensional deformation. In this model, deformation rates sharply decreased around 11.5 Ma when Bare Mountain rose along the Bare Mountain Fault and isolated the low-angle extensional fault system at Yucca Mountain from the more rapidly extending area west of Bare Mountain. This model does not directly include consideration of volcanism linked with extension and faulting.

Timing of volcanic events in the vicinity of Yucca Mountain has been addressed by Crowe (1990). He recognized older postcaldera basalts (OPB) between 9 and 6.3 Ma, all of which occur north or east of Yucca Mountain; and younger postcaldera basalts (YPB) between 3.7 Ma to Late Pleistocene, most of which (except two sites at Buckboard Mesa) occur south or west of Yucca Mountain. No basalt units were found to occur in the age range of 3.7 to 6.3 Ma, although there is an older episode of basaltic activity between about 11.5 and 8.5 Ma, approximately coincident with cessation of silicic volcanism in the Yucca Mountain region.

Crowe (1990) reports that mafic volcanic vents of southeast Crater Flat are probably aligned along and controlled by north-trending faults. At least four scoria cones and lava centers are associated with this field. The four Quaternary basalt centers comprising the 1.2-Ma alignment of central Crater Flat are, from northeast to southwest, an unnamed northeast cone, Black Cone, Red Cone, and Little Cones. These vents form a northeast-trending, arcuate alignment that suggests control of surface location of vents in central Crater Flat by the northeast-trending fault system at Yucca Mountain. The Sleeping Butte basalts

consist of two scoria cones and associated flows which define a northeast-trending alignment; Little Black Peak to the south, and Hidden Cone to the north.

The Crater Flat Volcanic Zone (CFVZ) of Crowe (1990) is defined by including all (young post-caldera basalts) YPB, except Buckboard Mesa, into a northwest-elongate zone. This zone was first defined by Crowe and Perry (1989). Crowe (1990) and Crowe et al. (1992) suggest that second-order northeast oriented structural trends within the CFVZ are reflected in the tendency of basalt centers in the CFVZ to form northeast-trending alignments of coeval or near-coeval age. Crowe et al. (1992) suggest the alignments may represent northeast-trending dike sets formed parallel to the direction of maximum horizontal compressive stress, which is the preferred direction of propagation of a dike in the *in situ* stress field. This concept relating chains of volcanic vents to stress pattern agrees with that proposed by Nakamura (1977) and Zoback (1992) where trend of the alignment should be perpendicular to minimum principal compressive stress. Zoback (1992) draws the analogy to a natural hydraulic fracture process in which the fluid pressure is due to magma rather than water. This concept may imply a temporal connection between extension and volcanism since the northeastern trend of vents described by several workers (Crowe, 1990; Crowe et al., 1992; Smith et al., 1990; Naumann et al., 1991) parallels normal faulting in the Yucca Mountain area. However, the exact relationships between volcanism and extension remain unresolved at present, and no models at the Yucca Mountain scale exist to adequately explain this relationship. Also, there are no mapped faults in the CFVZ with which the basaltic vents of this zone are exactly coincident. The CFVZ itself is parallel to structural elements of the northwest-trending Walker Lane belt, suggesting to Crowe et al. (1992) that basalt centers may be located along a buried structure or strike slip fault of the Walker Lane system.

Smith et al. (1990) consider north-northeast, north-northwest, or north-trending high-angle normal faults to control locations of volcanic centers in the Yucca Mountain area. These normal faults reflect the northeast direction of the regional trend of the Death Valley-Pancake Range Volcanic Belt. For central Crater Flat, Smith et al. (1990) observed that Black Cone has vents that occur along two subparallel zones striking about N35E, associated dikes also parallel this trend. Red Cone is comprised of three vent zones, two trending about N45E, and one about N50W. From Black Cone to Little Cones, Smith et al. (1990) indicate vent alignments show a 15° clockwise rotation. Rosenbaum et al. (1991) present paleomagnetic evidence that indicates the southern tip of Yucca Mountain was rotated about 30° clockwise relative to the northern part of the mountain after emplacement of the Tiva Canyon Member of the Paintbrush Tuff (i.e., post 13 Ma). The observed rotation may be a result of vertical-axis flexure over a deep-seated right lateral shear zone related to differential extension in hanging wall rocks across a regional detachment system (Rosenbaum et al., 1991). Lathrop Wells Cone is interpreted by Smith et al. (1990) to have formed along a splay of northeast-trending Solitario Canyon fault. Therefore, in their interpretation, structures controlling the location of volcanic vents in central Crater Flat and at Lathrop Wells are a part of the same northeast-trending fault system that both cuts and bounds Yucca Mountain. Naumann et al. (1991) indicate basaltic vents at Buckboard Mesa were primarily controlled by northeast-trending faults, although the eruptions were apparently focused at the intersection of the northeast-striking fault zone and the ring fracture zone of the Timber Mountain caldera. According to Naumann et al. (1991), Scrugham Peak cinder cone and several small vents occur along a main vent zone that is 1 km long, trends northeast, and is controlled by an echelon fault segments striking N10E. Crowe et al. (1992) reports vent zones of Buckboard Mesa are not located along northeast-trending structures, but along a 2 km long fissure oriented northwest.

3.2 IMPLICATIONS OF THE THEORETICAL MODELS

Overall, types of calculations presented in Section 2 do not provide definitive answers for site specific cases. Significant uncertainties exist with respect to rock properties and the physics of dike propagation. The real value of these calculations is to test assumptions, to identify important phenomena and key parameters, and to determine the trends of the results as functions of those key parameters.

Clearly the angle of the fault is an important parameter as well as the depth of the intersection with the fault. Other important parameters are the ductility, shear strength, and compressibility of the media because they determine the stiffness of the media and its ability to carry tensile stresses. In terms of the models, the horizontal displacement of the dike interface is dependent on the magma pressure. The pressure required for a given displacement is dependent on the stiffness of the media and the overburden stress. For the media used in these calculations, the dike pressure required was between three to four times the overburden stress. The three calculations comprising this study constrained the maximum dike opening (width) to about 1 m. Greater widths would require either higher dike pressures or a more compressible and lower strength rock media. Higher dike pressures may favor the continuation of the dike past the intersection, while a less stiff media may favor opening of the fault. There seems to be a definite leverage effect whereby the expanding fracture below the dike tip contributes to tensile stresses at the tip. It essentially acts as a lever to pry the tip open. This effect increases the distance that the fracture can move ahead of the pressure pulse. This phenomenon is a potentially important one that seems to be proportional to the length of the dike segment that is pressurized and inversely proportional to the tensile strength of the host rock. The media properties were taken from measurements on samples from the Yucca Mountain area, but the interpretation of the mechanical test data could have supported use of a less stiff media. Thus dike width could have been increased, and may have played a more important role in causing the fault to open.

At this time, only three relatively coarsely zoned calculations have been completed. The 60° fault at the 1-km depth showed both the fault and dike opening such that either path seemed likely to accommodate magma ascent. The calculation for the 80° fault at 1 km showed a slight opening of the dike a short distance from the intersection and relatively large opening of the fault such that the fault seemed the more likely path for the magma. The calculation for the 80° fault at 300 m showed only the fault opening up and, thus, serving as the only possible path for the magma.

Results of this study are generally in agreement with analytical modeling results (Connor et al. 1993) in that cohesionless faults with dips in excess of 60° are capable of acting as conduits for magma ascent in the depth range considered. However, a greater range of fault dips needs to be considered, and fault strength needs to be added to the dynamic models. Surface geological investigations and models of subsurface fault shape indicate that faults at Yucca Mountain are likely to maintain dips in excess of 60° throughout the depth range considered in this study (up to 1 km). Under environmental conditions specified for the dynamic models, faults that may be characterized as relatively simple contacts must be considered as potential conduits for magma ascent in this depth range. Probability and consequence estimates for mafic magmatic processes should include models that accommodate magma transport along fault zones.

4 REFERENCES

- Allmendinger, R.W., T.A. Hauge, E.C. Hauser, C.J. Potter, S.L. Klemperer, K.D. Nelson, P. Knuepfer, and J. Oliver. 1987. Overview of the COCORP 40 degree N transect, Western United States: The Fabric of an Orogenic Belt. *Geological Society of America Bulletin* 98(3): 308-319.
- Carr, M. 1984. Regional structural setting of Yucca Mountain, southwestern Nevada, and late cenozoic rates of tectonic activity in part of the southwestern Great Basin, Nevada and California. *U.S. Geological Survey Open File Report*. OF-84-854 Denver, CO: U.S. Geological Survey: 109.
- Champion, D.E. 1991. Volcanic episodes near Yucca Mountain as determined by paleomagnetic studies at Lathrop Wells, Crater Flat, and Sleeping Butte, Nevada. *Proceedings of Second Annual International Conference on High Level Radioactive Waste Management*. La Grange Park, IL: American Nuclear Society: 61-67.
- Coney, P.J. 1973. Non-collision tectogenesis in western North America. *Implications of Continental Drift to the Earth Sciences*. D.H. Tarlin and S.H. Runcorn, eds. New York City, NY: Academic Press: 713-727.
- Connor, C.B., S. McDuffie, and B.E. Hill. 1994. *NRC High-Level Radioactive Waste Research at CNWRA, July - December 1993*. Chapter 10: Field Volcanism Research. CNWRA 93-02S. San Antonio, TX: Center for Nuclear Waste Regulatory Analyses: 10-1 to 10-26.
- Connor, C.B., and B.E. Hill. 1993. *NRC High-Level Radioactive Waste Research at CNWRA, July 1 through December 31, 1992*. Chapter 10: Volcanism Research. NRC-02. W.G. Mook and H.T. Waterbolk, eds. 88-005. Washington, DC: Nuclear Regulatory Commission: 10-1 to 10-31.
- Crowe, B.M., and F.V. Perry. 1989. Volcanic probability calculations for the Yucca Mountain site: Estimation of volcanic rates. *Proceedings of Nuclear Waste Isolation in the Unsaturated Zone, Focus '89*. La Grange Park, IL. American Nuclear Society: 326-334.
- Crowe, B.M. 1990. Basaltic volcanic episodes of the Yucca Mountain region. *Proceedings of High-Level Radioactive Waste Management, International Conference*. La Grange Park, IL: American Nuclear Society 1: 65-73.
- Crowe, B.M., R. Picard, G. Valentine, and F.V. Perry. 1992. Recurrence models for volcanic events: Applications to volcanic risk assessment. *Proceedings of Third Annual International Conference on High-Level Radioactive Waste Management*. La Grange Park, IL. American Nuclear Society: 2: 2,344-2,355.
- Emmerman, S.H. and R. Marrett. 1990. Why dikes? *Geology* 18: 231-233.

- Hamilton, W.B. 1988. Detachment faulting in the Death Valley region, California and Nevada. M.D. Carr and J.C. Yount, eds. *Geologic and Hydrologic Investigations of a Potential Nuclear Waste Disposal Site at Yucca Mountain, Southern Nevada. U.S. Geological Survey Bulletin 1790*, Denver, CO: U.S. Geological Survey: 51–85.
- Ho, C.-H. 1992. Risk assessment for the Yucca Mountain high-level nuclear waste repository site: Estimation of volcanic disruption. *Mathematical Geology* 24: 347–364.
- Kruse, S.M., M. McNutt, J. Phipps-Morgan, L. Royden, and B. Wernicke. 1991. Lithospheric extension near Lake Mead, Nevada: A model for ductile flow in the lower crust. *Journal of Geophysical Research* 96(B3): 4,435–4,456.
- Kuntz, M.A. 1992. A model-based perspective of basaltic volcanism, eastern Snake River Plain, Idaho, in P.K. Link, M.A. Kuntz, and L.B. Platt, eds., *Regional Geology of Eastern Idaho and Western Wyoming: Geological Society of America Memoir 179*: 289–304.
- Nakamura, K. 1977. Volcanoes as possible indicators of tectonic stress orientation – principles and proposal. *Journal of Volcanology and Geothermal Research* 2: 1–16.
- Naumann, T.R., D.L. Feuerbach, and E.I. Smith. 1991. Structural control of Pliocene volcanism in the vicinity of the Nevada Test Site, Nevada: An example from Buckboard Mesa. *Geological Society of America Abstracts*. Boulder, CO: Geological Survey of America: 23(2): 82.
- Okaya, D.A., and G.A. Thompson. 1986. Involvement of deep crust in extension of nasin and range province in extensional processes and kinematics. L. Mayer, ed. *Geological Society of America Special Paper 208*. Boulder, CO: *Geological Society of America* 15–22.
- Parsons, T., and G.A. Thompson. 1993. Does magmatism influence low-angle normal faulting? *Geology* 21: 247–250.
- Parsons, T., and G.A. Thompson. 1991. The role of magma overpressure in suppressing earthquakes and topography: World-wide examples. *Science* 253: 1,399–1,402.
- Petford, N., R.C. Kerr, and J.R. Lister. 1993. Dike transport of granitoid magmas. *Geology* 21: 845–848.
- Pollard, D.D. 1987. Elementary fracture mechanics applied to the structural interpretation of dykes in mafic dike swarms. H.C. Halls and W.F. Fahrig, eds., *Geological Association of Canada Special Paper 34*: 5–24.
- Pollard, D.D., and P. Segall. 1987. *Theoretical Displacements and Stresses Near Fractures in Rock: With Applications to Faults, Joints, Veins, Dikes, and Solution Surfaces, Fracture Mechanics of Rock*. Atkinson, B.K., ed. San Diego, CA: Academic Press: 277–350.
- Reheis, M.C. 1986. Preliminary study of Quaternary faulting on the east side of Bare Mountain, Nye County, Nevada. *U.S. Geological Survey Open File Report OF-86-576*, Denver, CO: U.S. Geological Survey: 24.

- Rosenbaum, J.G., M.R. Hudson, and R.B. Scott. 1991. Paleomagnetic constraints on the geometry and timing of deformation at Yucca Mountain, Nevada. *Journal of Geophysical Research* 96(B2): 1,963–1,979.
- Scott, R.B. 1990. Tectonic setting of Yucca Mountain, southwestern Nevada, Basin and Range Extensional Tectonics Near the Latitude of Las Vegas, Nevada. B.P. Wernicke, ed. *Geological Society of America Memoir* 176: 251–282.
- Scott, R.B., and J. Bonk. 1984. Preliminary geologic map of Yucca Mountain, Nye County, Nevada, with geologic sections. *U.S. Geological Survey Open File Report* 84-494, Denver, CO: U.S. Geological Survey: 1: 12,000.
- Scott, R.B., and J. Whitney. 1987. The upper crustal detachment system at Yucca Mountain, SW Nevada. *Geological Society of America Abstracts with Programs* 19: 332–333.
- Smith, E.I., T.R. Feuerbach, and J.E. Faulds. 1990. The area of most recent volcanism near Yucca Mountain, Nevada: Implications for volcanic risk assessment. *Proceedings of the International Topical Meeting on High Level Radioactive Waste Management*. La Grange Park, IL: American Nuclear Society 1: 81–90.
- Stewart, J.H. 1984. Basin-range structure in western North America: A review. Cenozoic tectonics and regional geophysics of the western Cordillera. R.B. Smith and G.P. Eaton, eds. *Geological Society of America Memoir* 152: 1–31.
- Swadley, W.C., D.L. Hoover, and J.N. Rosholt. 1984. Preliminary report on late Cenozoic stratigraphy and faulting in the vicinity of Yucca Mountain, Nye County, Nevada *U.S. Geological Survey Open File Report* OF-84-788: Denver, CO: U.S. Geological Survey: 42.
- Turrin, B.D., and D.E. Champion. 1990. $^{40}\text{Ar}/^{39}\text{Ar}$ laser fusion and K-Ar ages from Lathrop Wells, Nevada, and Cima, California: The age of the latest volcanic activity in the Yucca Mountain area. *Proceedings of International Topical Meeting on High Level Radioactive Waste Management*. La Grange Park, IL: American Nuclear Society: 68–5.
- Van Burkirk, R.G., D.S. Gardiner, and S.W. Butters. 1978. Characterization of Yucca Flat materials. *Terra Tek Report* 78-67. Salt Lake City, UT: Terra Tek Inc.: 38.
- Wernicke, B.P., G.J. Axen, and J.K. Snow. 1988. Basin and Range extensional tectonics at the latitude of Las Vegas, Nevada. *Geological Society of America Bulletin* 100: 1,738-1,757.
- Whirley, R.G., and J.O. Hallquist. 1991. DYNA3D A nonlinear, explicit, three-dimensional finite element code for solid and structural mechanics – user manual. *UCRL-MA-107254*. Livermore, CA: Lawrence Livermore National Laboratory.
- Young, S.R., G. Stirewalt, and A. Morris. 1993. *Geometric Models of Faulting at Yucca Mountain*. Dynamic Analysis and Design Considerations for High-Level Nuclear Waste Repositories. Hossain, Q.A., ed. New York City, NY: American Society of Civil Engineers: 97–115

Zoback, M.D. 1992. First and second-order patterns of stress in the lithosphere: The world stress map project. *Journal of Geophysical Research* 97(B8): 11,703–11,728.